$x$ = cartesian coordinate
$x$ = progress variable
$x_j$ = $j$th moment of size distribution of growing polymer chains
$x'$, $x''$ = dummy variables
$y$ = cartesian coordinate
$y$ = progress variable
$y_j$ = $j$th moment of size distribution of terminated polymer
$y'$, $y''$ = dummy variables
$z$ = cartesian coordinate

**Greek Letters**

$\alpha$ = inverse of nominal residence time
$\beta$ = measure of agglomerative mixing intensity
$\epsilon$ = actual power input to mixing system per unit mass of fluid
$\eta$ = empirical efficiency parameter
$\lambda$ = mixing intensity parameter, $= 2\beta/\alpha$
$\mu$ = mean concentration
$\mu_0$ = mean feed concentration
$\mu_n$ = $n$th moment of $p$
$\mu_{n;0}$ = $n$th moment of $p_0$
$\mu_n^j$ = $n$th moment of $p^j$
$\nu$ = kinematic viscosity of working fluid
$\nu$ = number of radicals formed by each molecule of decomposing initiator
$\sigma^2$ = variance of concentration distribution
$\sigma_0^2$ = variance of feed distribution
$\tau$ = mean residence time
$\tau_m$ = mixing time
$\phi$ = concentration distribution of growing polymer chains
$\psi$ = concentration distribution of terminated polymer

**LITERATURE CITED**


1. Batchelor, G. K., *J. Fluid Mech.*, **5**, 113 (1959).
2. Brodkey, R. S., and J. O. Nye, *Rev. Sci. Instr.*, **34**, 1086 (1963).
   ———, and J. Lee, *AIChE J.*, **10**, 187 (1964).
3. Corrsin, S., *ibid.*, **3**, 329 (1957); **10**, 870 (1964).
4. Curl, R. L., *AIChE J.*, **9**, 175 (1963).
5. Kim, Y. G., and R. H. Wilhelm, Preprint 26B, Fifty-sixth Annual Meeting of the AIChE, Houston, Texas.
6. Rietema, K., *Advan. Chem. Eng.*, **5**, (1964).
7. Shain, S., *AIChE J.*, **12**, 806 (1966).
8. Shinnar, R., *J. Fluid Mech.*, **10**, Pt. 2, 259 (1961).
9. ———, and J. M. Church, *Ind. Eng. Chem.*, **52**, 253 (1960); **53**, 479 (1961).
10. Spalding, D. B., *Combustion Flame*, **1**, 287, 296 (1957).
11. Spielman, L. A., and O. Levenspiel, *Chem. Eng. Sci.*, **20**, 247 (1965).
12. Tadmor, Z., and A. Biesenberger, *Ind. Eng. Chem. Fundamentals*, **5**, 336 (1966).
13. Van de Vusse, J. G., *Chem. Eng. Sci.*, **4**, 178, 209 (1955).
14. *Ibid.*, **17**, 507, 1962.
15. Weinstein, H., and R. J. Adler, *Chem. Eng. Sci.*, **22**, 65 (1967).
16. Worrell, G. R., and L. C. Eagleton, *Can. J. Chem. Eng.*, **43**, 254 (Dec. 1964).
17. Zwietering, Th. N., *Chem. Eng. Sci.*, **11**, No. 1, 1 (1959).
18. Kattan, A., and R. J. Adler, *AIChE J.*, **13**, 580 (1967).
19. Saidel, G. M., and S. Katz, *ibid.*, 319 (1967).


*Manuscript received October 11, 1967; revision received June 26, 1968; paper accepted July 18, 1968.*

# The Dynamic Modeling, Stability, and Control of a Continuous Stirred Tank Chemical Reactor

**W. FRED RAMIREZ and BRIAN A. TURNER**

**University of Colorado, Boulder, Colorado**

***A realistic CSTR model was developed and verified experimentally. The reaction studied was the exothermic, base sodium hydroxide catalyzed decomposition of hydrogen peroxide. The model was used to evaluate the usefulness of the following stability analyses: steady state analysis, local linearization and Liapunov's direct method through Krasovskii's theorem. The effect of control valve hysteresis on the system was also investigated.***

The purpose of this investigation was to study both experimentally and theoretically the dynamics and control of a continuous stirred tank reactor, a C.S.T.R. There exist several analytical methods for determining stability in a C.S.T.R. (*1* to *4*, *7*). These include steady analysis (*7*), linearization techniques (*3*), and Krasovskii's Theorem with the Liapunov function it suggests (*2*).

Brian A. Turner is now with the Shell Oil Company, Martinez, California.

## DYNAMIC EQUATIONS

The system considered was a continuous stirred tank reactor. The reaction was first order and homogeneously catalyzed. The reactant, hydrogen peroxide, and the catalyst, sodium hydroxide, were fed into the reactor, while the product, water, and unreacted peroxide were continuously removed. The solution density and heat capacity varied with concentration, but their product is nearly constant and was considered constant in formulating the dynamic model. The exothermic heat of reaction was continuously removed through a cooling water belt which

TABLE 1.

| | |
|---|---|
| $A = 3.18$ sq. ft. | $G_{max} = 20$ ma. |
| $C_0 = 11.5$ g.moles/liter | $H = 22.6$ K cal./mole |
| $C_2 = 0.1068$ ma./°K. | $T_0 = 22$°C. |
| $C_1 = 62.5$ (B.t.u./hr. sq. ft. °F.)/(lb./min.)$^{1/3}$ | $T_{ss} = 30$°C. |
| $c_p = 0.865$ cal./°K. g. | $T_{in} = 10$°C. |
| $c_{p_{coolant}} = 1$ cal./°K. g. | $V = 16.2$ liters |
| $F_0 = 0.5$ liters/min. | $\rho = 1.1081$ g./cc. |
| $G_{min} = 4$ ma. | |

surrounded the reactor. The following mass and energy balances describe the C.S.T.R.
Energy Balance:

$$\rho V c_p \frac{dT}{dt} = H\,Vk(T)\,C - UA(T - T_A) - \rho F_0 c_p\,(T - T_0) \quad (1)$$

Material Balance:

$$V\frac{dC}{dt} = -Vk(T)\,C - F_0\,(C - C_0) \quad (2)$$

The heat removal driving force term involving $(T - T_A)$ is modeled by assuming that the cooling water temperature in the belt is an arithmetic average of the input and output cooling temperatures. Employing this assumption and an energy balance across the cooling water belt gives,

$$(T - T_A) = \frac{T - T_{in}}{1 + 1/F} \quad (3)$$

where

$$F = \frac{2\,Q_c\,c_p}{UA}$$

For laminar flow the overall transfer coefficient is related to the mass flow rate coolant according to Equation (4).

$$U = C_1\,Q_c^{1/3} \quad (4)$$

where $C_1$ = constant
The functional relationship between the mass flow rate of coolant and the controller output is usually given by the controller manufacturer, or can be determined experimentally. Figure 1 is the control valve characteristic curve which was determined experimentally. This figure shows that the control valve exhibited valve hysteresis. The fraction controller output is related to the proportional gain through Equations (5) and (6).

$$c = \frac{G - G_{min}}{G_{max} - G_{min}} \quad (5)$$

$$G = -K(T - T_{ss})\,C_2 + C_3 \quad (6)$$

Values of the various variables and constants which were used in this study are given in Table 1.

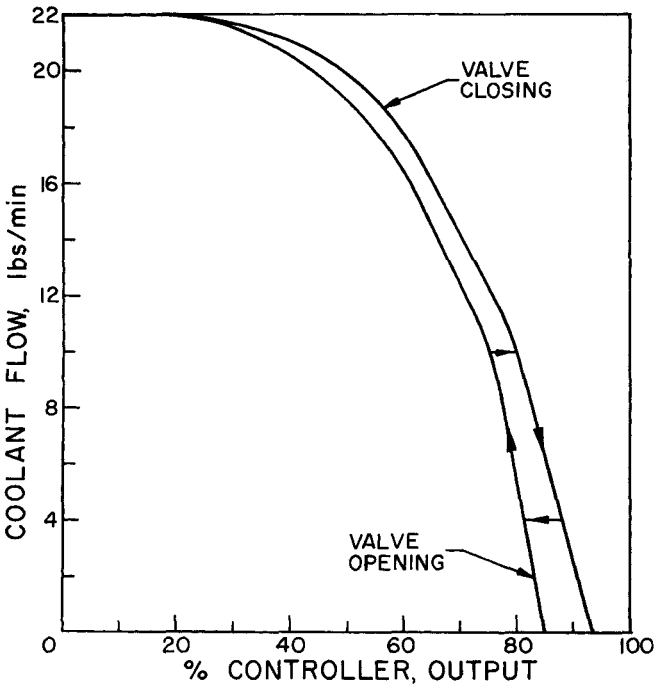

Fig. 1. Control valve characteristic.

## PRESENT WORK

To conserve chemicals, the experimental reactor was run as a batch rather than a continuous process. Since the mixing terms had to be removed from the model to represent a batch reactor, ideality of the mixing of the experimental reactor was evaluated by a separate mixing experiment. Initial estimates of the reaction kinetics were calculated from literature data (5) and steady state reaction experiments.

The system equations were then modeled on the Beckman 2200—SDS 920 hybrid computer. The nonlinear functions and first derivatives of temperature and concentration were calculated continuously on the digital computer while the temperature and concentration responses were produced by integrating the derivatives on the analog computer.

To verify the computer solution of the model, experimental temperature and concentration responses were obtained by operating the actual C.S.T.R. as a batch reactor. At this time everything in the model except the reaction kinetics had been defined. Steady state experimental data gave good estimates of the reaction rate constants at certain temperatures, while the literature (8) gave an estimate of the Arrhenius temperature dependency. Using the initial estimate of the reaction kinetics, the model solution was made to fit the experimental dynamic results by manipulating the frequency factor and activation energy terms in the Arrhenius kinetics. Independent experimental dynamic data was then taken to define the predictive ability of the model.

Once the correct mathematical model of the reactor and control system was verified, the stability analyses were applied to the model.

## EXPERIMENTAL APPARATUS AND PROCEDURE

The equipment used in this study consisted of a batch tank reactor, standard industrial feedback-control equipment, and

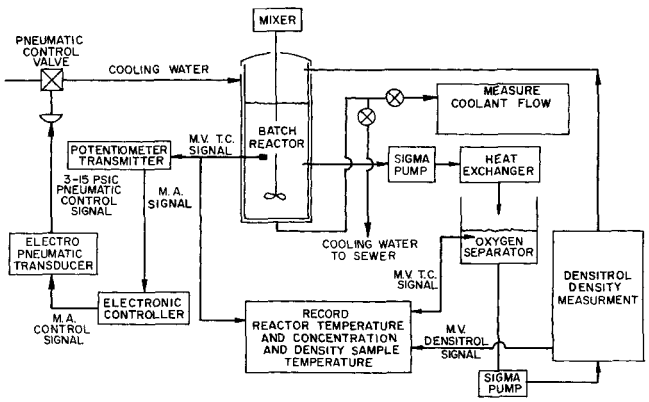

Fig. 2. Batch reactor system flow sheet.

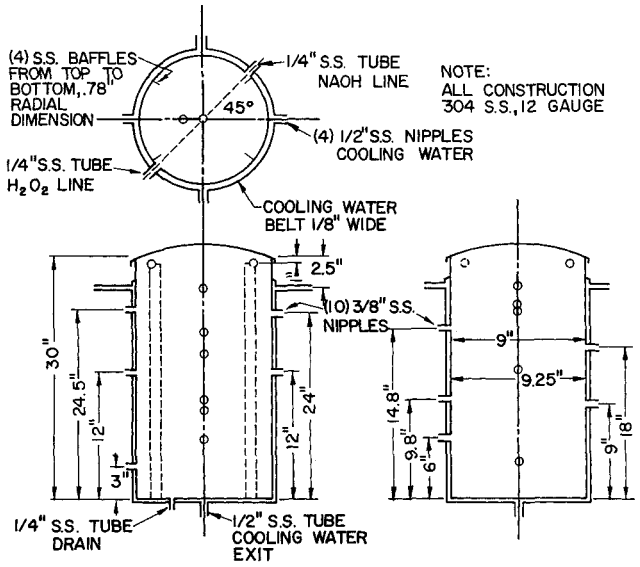


**Fig. 3. Tank reactor.**

commercially-purchased instrumentation to measure the temperature and concentration responses. A flow diagram of the integrated system is given in Figure 2.

The hydrogen peroxide reactant and the sodium hydroxide catalyst were well agitated in the tank reactor (Figure 3) by a one-eighth horsepower Lightnin' mixer with a three-blade, 4 in. propeller of 1.15 pitch, centered 6 in. above the bottom of the tank.

The reactor itself was fabricated entirely of 12 gauge, 304 stainless steel, with all joints welded. Located at random about the periphery of the tank were ten ⅜ in. 304 stainless steel nipples welded to the inside wall and soldered to the outside wall. These ⅜ in. nipples were included to give various sampling points, holding times and thermocouple positions. The cooling water entered the top of the cooling belt through four ½ in. 304 stainless steel tubes, equally spaced about the periphery. The coolant was removed from a single ½ in. tube centered at the bottom of the reactor.

The reactor temperature was controlled by manipulating the cooling water flow rate. The reactor temperature was continuously sensed by a stainless steel sheathed iron constantan thermocouple reference to an ice bath. The millivolt thermocouple signal was converted to a 4 to 20 ma. transmission signal through the use of Taylor potentiometer transmitter. A Taylor three-mode electronic controller-recorder recorded the temperature and produced a 4 to 20 ma. control signal. To initiate control, a Fisher Governor electro pneumatic transducer converted a milliamp control signal to a 3 to 15 lb./sq. in. gauge pressure signal. The pneumatic signal operated a Taylor quick-opening flow valve through a Taylor Lin-E-Air actuator.

The concentration of hydrogen peroxide in the reactor was measured by continuously measuring the density with a Princo densitrol. Since the reactor was continuously releasing oxygen gas, any density measurements were inaccurate. The density sample drawn from the reactor was cooled to 10°C. Cooling the solution extinguished the reaction and stopped the evolution of oxygen. The sample then entered a 200 ml. separatory funnel which acted as a gas-separation unit. The sample was then delivered to the Princo densitrol ,where the density was continuously measured, and then returned to the reactor.

## RESULTS

### Model

The temperature and concentration responses of the experimental reactor compared favorably with those predicted from the solution of the model (Figures 4, 5). The experimental data is the result of mixing 4.75 N sodium hydroxide and 50% hydrogen peroxide in the batch reactor. The Arrhenius temperature-dependency of the

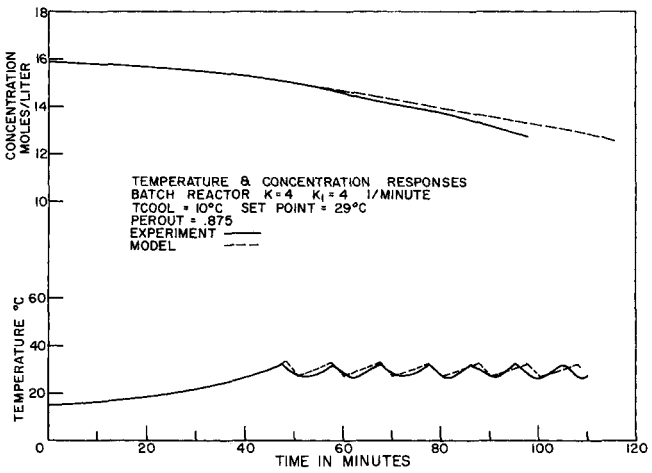


**Fig. 4. Run 1.**

chemical kinetics was found from the literature to be approximately

$$k(T) = 6.3 \times 10^{10} e^{-9{,}250/T} \tag{7}$$

The dynamic responses of the model were fit to the first experimental response (Figure 4) by manipulating the kinetic rate constant into the form

$$k(T) = 5.04 \times 10^{10} e^{-9{,}310/T} \tag{8}$$

This represents a 21% change in the frequency factor and a 0.6% change in the activation energy. These percent deviations were within the experimental error of the estimates. Figure 4 shows that the experimental concentration curve decreases faster than the model after 58 min. have lapsed. This discrepancy is caused because there is a slight loss of volume from the decomposition reaction of hydrogen peroxide. The volume loss increases the catalyst concentration and therefore increases the reaction rate. Further evidence of the increased reaction rate is the increase in the slope of the temperature curve as a function of time, which leads to ever shortening the temperature cycles. This loss of volume was not considered in the model.

The second experimental response (Figure 5) was considered to illustrate the predictive ability of the model. The controller constants in this run were varied significantly. The model was operated with the kinetics of the first run. The experimental temperature response (Figure 5) reached its first peak some 4 min. later than the model did. This response error was caused by slight errors, within 1°C., in measuring the initial temperature. Initial temperature errors were enlarged by integration over large time periods. Dynamic-response errors due to measurement error introduce very serious problems when the control action depends upon some initial state measurements and the system model. Time-displaced errors would necessitate frequent sampling of the state variables in control policies using optimal control or feed-forward techniques.

The experimental temperature response, other than being displaced in time from the model response, is within 1 min. and 2°C. of the model with regard to frequency and amplitude of oscillation. The increased slope of the last experimental temperature cycle (Figure 5) and the increasing slope of the experimental concentration curve at this time both indicate that the reaction rate is speeding up toward the end of the run due to volume losses.

Runs were made to show that the experimental procedure used was reproducible. The temperature and concentration responses were shown identical within 2%

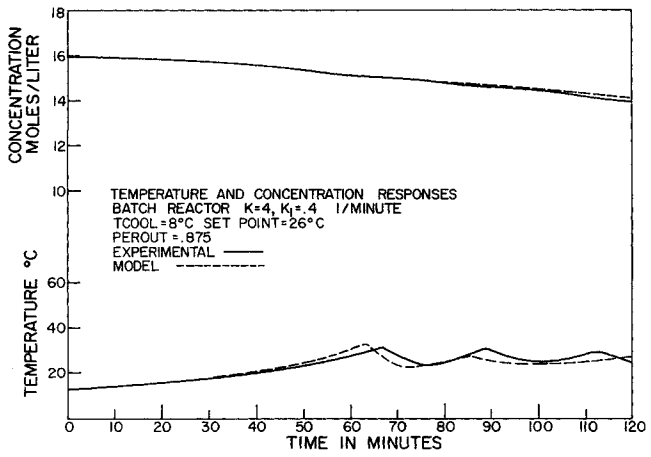


Fig. 5. Run 2.

error. The experimental work was accomplished in the sensitive area of the control valve operation. The controller setpoint of 87.5% output represented operation in the steepest portion of the control valve curve where the hysteresis was greatest. Therefore, any agreement between the model and the experimental responses in this region should confirm the validity of the model over the entire operation of the control valve. Working in an area of near instability meant that slight changes in the parameters of the model, such as lowering the set-point 1 or 2°C. would result in an entirely different temperature response. Therefore this work was carried out under conditions of sensitive process dynamics.

### Phase Plane

The phase plane representation involves plotting the two state variables, one as a function of the other with the independent variable, time, a parameter along the phase plane curves. The phase plane illustrates the concentration and temperature responses for all possible initial conditions of interest. The phase planes of the system model are shown in Figures 6 to 8. Figure 6, the phase plane for the reactor without control, indicates that all initial conditions with temperature greater than the set-point increase in temperature. Responses with initial conditions less than the set-point are initially drawn to the set-point temperature, then the temperature increases. Figure 7 shows a phase plane for a proportional controller gain $K = 1$, which is representative of the responses between $K = 0$ and $K = 3$. Increasing the gain up to 3 results in an unstable reactor with an operating point less than the desired 30°C. The off-set operating point is drawn closer to the set-point as the gain approaches 3.

Figure 8, for a gain equal to 5, is representative of all gains greater than 3. This phase plane clearly shows the temperature chatter about the set-point which is due to hybrid computer solution dynamics.

To isolate the effect of valve hysteresis, phase planes for the model programmed with only the valve opening curve were produced on the hybrid computer and are plotted in Figures 9 and 10. Figure 9 shows the phase plane for a gain $K = .015$. Here the singularity is unstable. Increasing $K$ to 1.0, Figure 10, results in a very stable phase plane. A comparison of Figures 10 and 7 shows the effect of neglecting valve hysteresis in the analysis. For a proportional gain of 1, the nonlinear phase plane with valve hysteresis shows that the system is not asymptotically stable, while the phase plane without hysteresis shows the system to be extremely asymptotically stable.

### Steady State Analysis

The heat production curve for the experimental reactor is shown in Figure 11. This curve is not sigmoid in shape as predicted by the general theory because boiling occurs before the upper half of the curve can be completed. The heat-removal term intersects the heat-production curve at 30°C. only. Therefore there was only one singular point for this system rather than the three which can be generally expected (7). The singular point at 30°C. is stable for negative temperature upsets and unstable for positive temperature upsets. The reactor phase plane without control (Figure 6) shows that all reactor responses with initial temperature responses less than the set-point are drawn to the singular point while all responses with initial temperatures greater than the set-point grow.

### Linear Analysis

The most straightforward method of specifying the amount of control necessary for reactor stability is achieved by analyzing linearized equations describing the system (3). The first step usually taken in this approach is to normalize the system about the steady state.

$$\hat{T} = T - T_{ss} \tag{9}$$

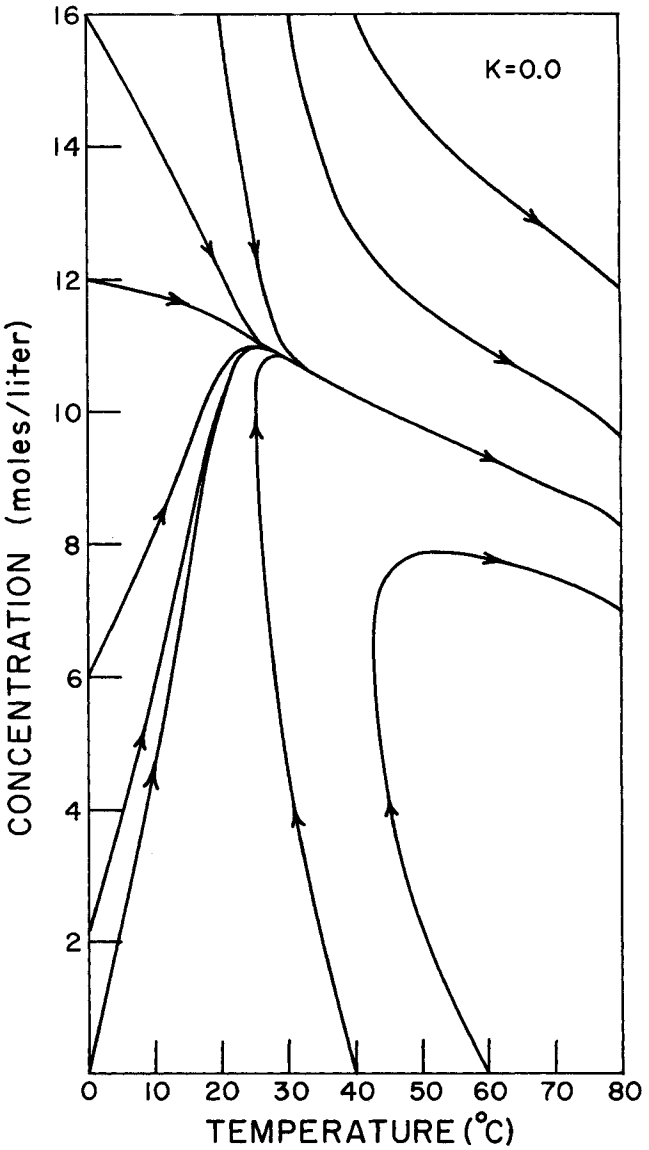


Fig. 6. Phase plane nonlinear system.

$$\hat{C} = C - C_{ss} \tag{10}$$

The next step is to expand the system equations describing temperature and concentration in a first-order Taylor series. This gives Equations (11) and (12).

$$\dot{\hat{C}} = -a_{11}\hat{C} - a_{12}\hat{T} \tag{11}$$

$$\dot{\hat{T}} = -a_{21}\hat{C} - (a_{22} + a_{23})\hat{T} \tag{12}$$

where

$E$ = activation energy

$$a_{11} = \left[\frac{F_0}{V} + k(T)\right]_{ss}$$

$$a_{21} = -\left[\frac{k(T)H}{\rho C_p}\right]_{ss}$$

$$a_{12} = \left[\frac{E\,k(T)C}{T^2}\right]_{ss}$$

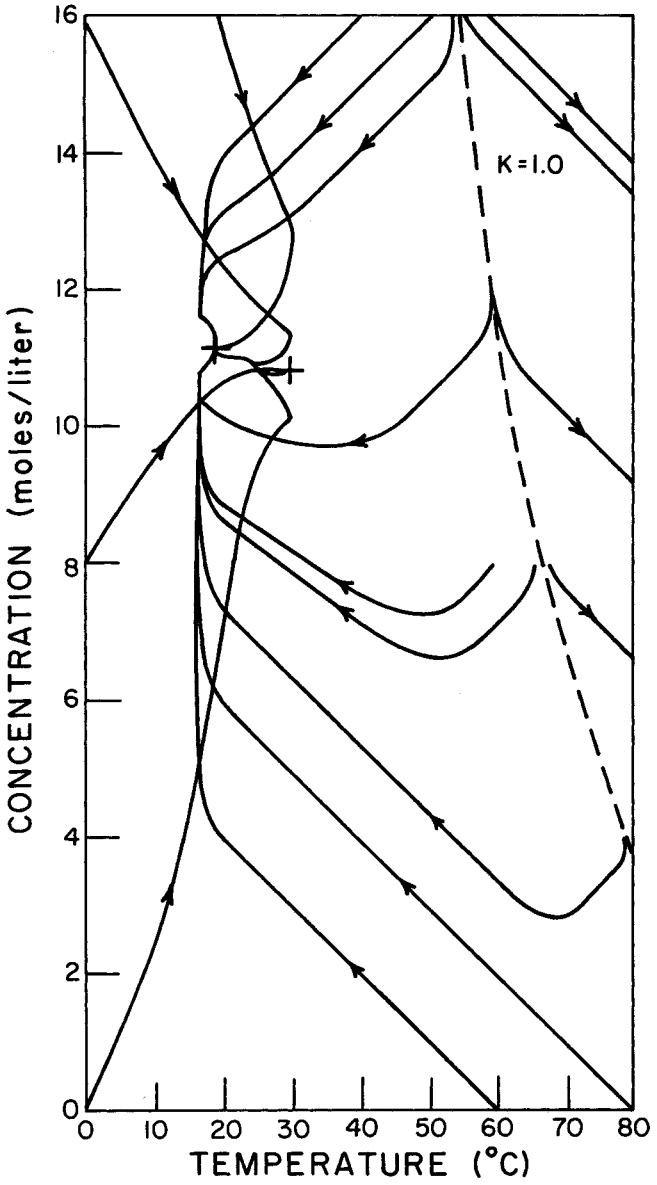


Fig. 7. Phase plane nonlinear system.

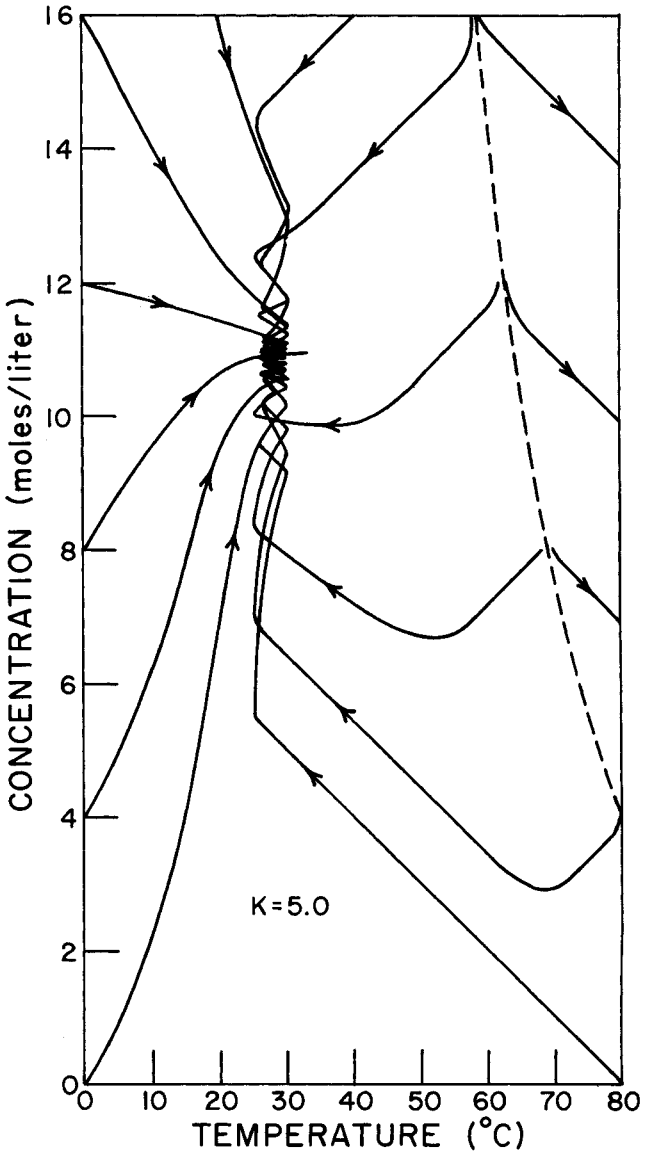


Fig. 8. Phase plane nonlinear system.

$$a_{22} = \left[\frac{F_0}{V} - \frac{E\,k(T)C}{T\,\rho\,c_p} + \frac{UA}{\rho\,V\,c_p(1 + 1/F)}\right]_{ss}$$

$$a_{23} = \left[\frac{A(T - T_{in})}{\rho\,C_p\,V}\,\frac{\partial\left(\dfrac{U}{1 + 1/F}\right)}{\partial T}\right]_{ss}$$

For the conditions of interest the linearized equations become

$$\dot{\hat{C}} = -0.0332\,\hat{C} - 0.00251\,\hat{T} \tag{13}$$

$$\dot{\hat{T}} = 0.0547\,\hat{C} + 0.0116\,\hat{T} - 0.498\,K\,\hat{T} \tag{14}$$

The roots of the characteristic equation of the linear system are of opposite sign; therefore the singular point is a saddle point. By increasing the gain above 0.015 the eigenvalues of the characteristic equation became real and negative, which indicated that the singular point had become a stable node. The phase plane resulting from solving the linear equation with $K = 0.015$, is shown in Figure 12.

The linearized equations are valid only in an extremely small region about the steady state. Stability calculated from the linearized equations is referred to as local stability. The gain constants obtained from the linear analysis can be considered only minimal at best. Further lack of confidence in the linear analysis should be drawn from the fact that the linearization process has no way to consider the valve discontinuities of hysteresis and saturation.

The phase plane of the nonlinear model without valve hysteresis, Figure 9, shows the linear analysis was not correct in predicting local stability for a gain of 0.015. The dynamics for the model with valve hysteresis shows asymptotic stability can not be achieved until the gain is greater than 3.0. The linear analysis was not effective in predicting stability for the nonlinear system.

#### Liapunov's Direct Method and Krasovskii's Theorem

Global asymptotic stability is guaranteed for any system if a scalar function, called the Liapunov function, with continuous first partial derivatives and the following characteristics can be found (2, 6):

$$V(\underline{x}) = 0 \text{ for } \underline{x} = 0 \tag{15}$$

$$V(\underline{x}) > 0 \text{ for } \underline{x} \neq 0 \tag{16}$$

$$V(\underline{x}) \to \infty \text{ as } ||\underline{x}|| \to \infty \tag{17}$$

$$\frac{dV}{dt}(\underline{x}) < 0 \text{ for } \underline{x} \neq 0 \tag{18}$$

where $\underline{x}$ represents the state vector, $V(\underline{x})$ represents a Liapunov function, and $||\underline{x}||$ represents the norm of the state vector.

The Liapunov approach to stability analysis again represents a situation in which stability can be studied without integrating the system equations. Since it is indeed a rare situation that produces global stability, we are generally trying to establish stability in defined regions. By applying Equations (15), (16) and (18), we can insure stability in a bounded region $V(\underline{x}) < K$.

There are several limitations to Liapunov's direct method. The restrictions for stability are sufficient but not necessary (7). In other words, if a Liapunov function cannot be found to insure stability for a region of interest, then the region is said to be indeterminate rather than unstable. Another limitation to the method is that there are no general methods for determining a Liapunov function for a system. A final limitation is that a system may have any number of Liapunov functions, some of which are better than others. Therefore, most results obtained through the use of this method would be conservative.

However, one important class of nonlinear equations can be treated systematically. If the system of equations can be written in the following form

$$\dot{\underline{x}} = \underline{f}(\underline{x}) \tag{19}$$

and

$$\underline{f}(\underline{0}) = \underline{0}$$

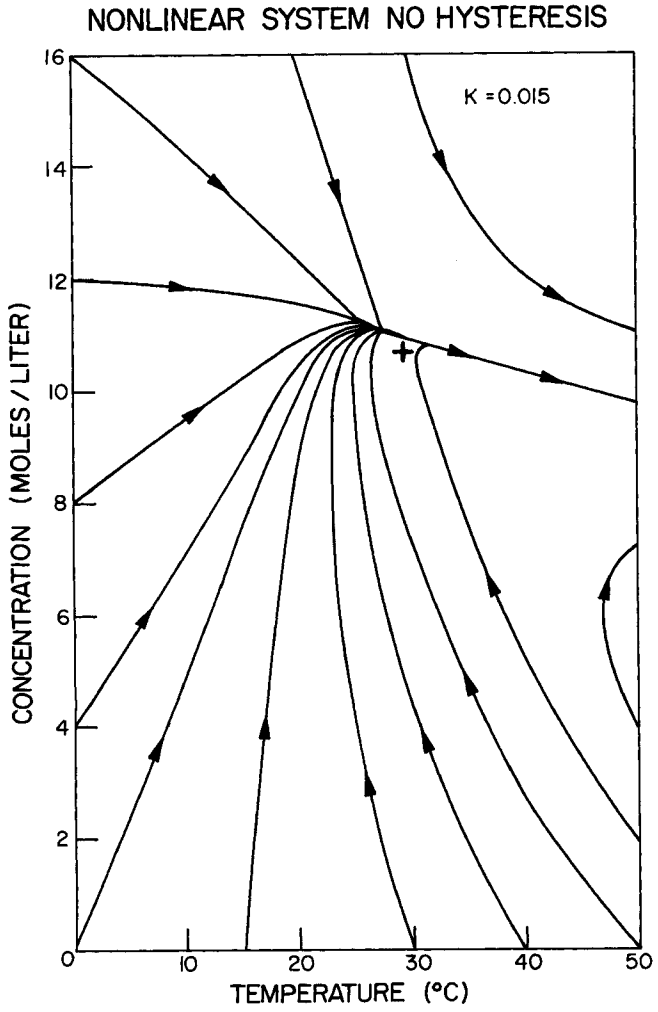


Fig. 9.

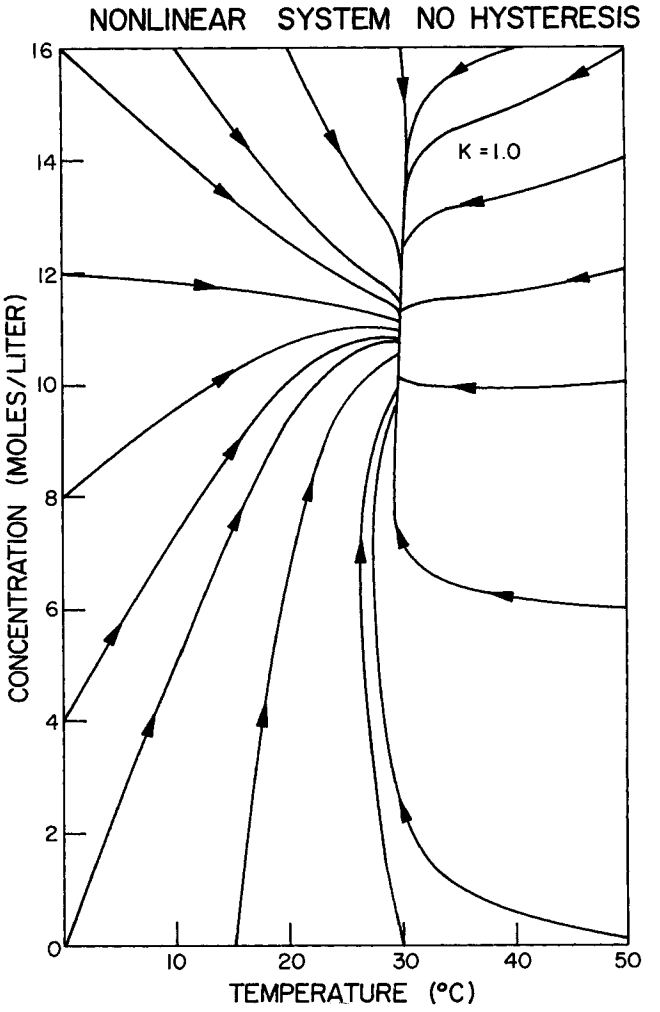


Fig. 10.

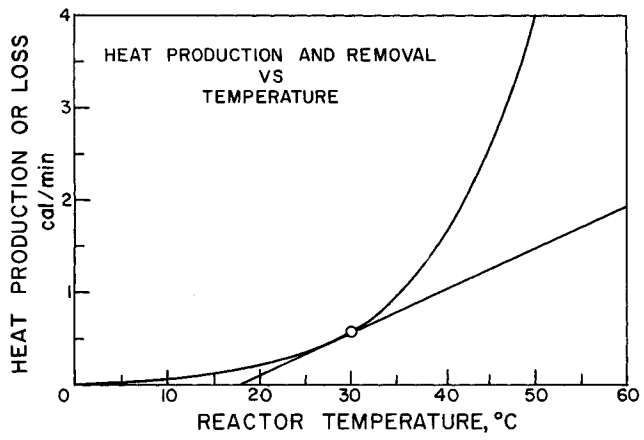


Fig. 11. Steady state analysis (real system).

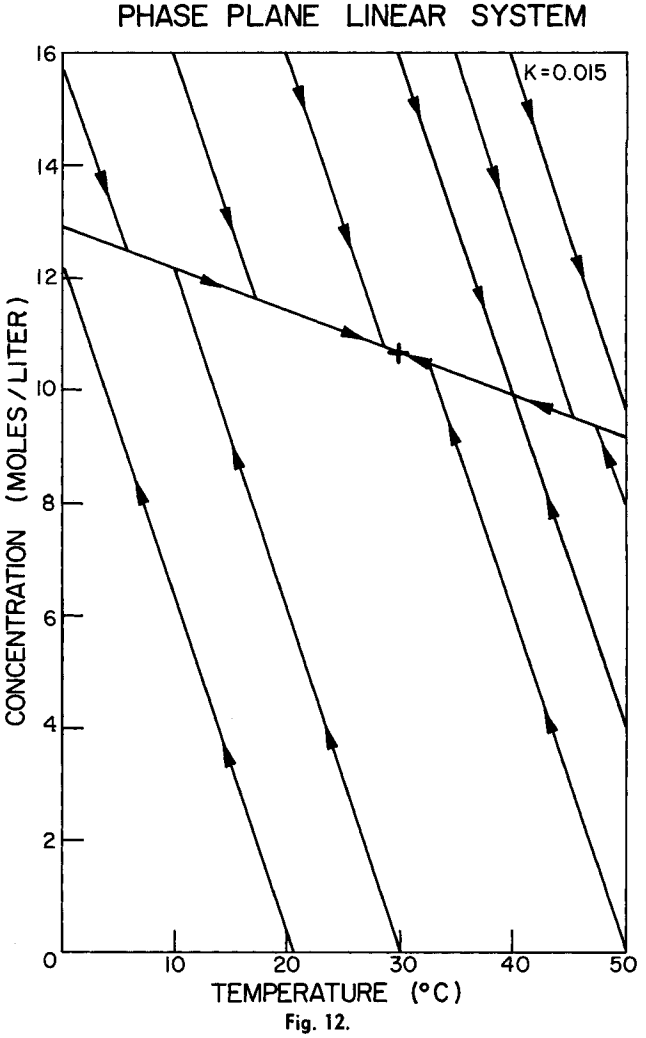


Fig. 12.

they are subject to Krasovskii's Theorem (2). If we let the Jacobian matrix be defined by

$$\underline{\underline{F}}(x) = [\partial f_i/\partial x_j] \tag{20}$$

and $\hat{\underline{\underline{F}}}(\underline{x})$ by

$$\hat{\underline{\underline{F}}}(\underline{x}) = \underline{\underline{F}}(\underline{x}) + \underline{\underline{F}}^T(\underline{x}) \tag{21}$$

where $T$ = the transpose of a matrix, then Krasovskii's Theorem states that if $\underline{f}$ has continuous first partials and if $\hat{\underline{\underline{F}}}(\underline{x})$ is negative definite then the steady state $\underline{x}_{ss} = \underline{0}$ of the system is asymptotically stable in the large, and

$$V(\underline{x}) = ||\underline{f}(\underline{x})||^2 \tag{22}$$

is a Liapunov function for the system.

In general, $\hat{\underline{\underline{F}}}(\underline{x})$ will not always be negative definite and when it is not, $||\underline{f}||^2$ functions which lie within the region bounded by $\hat{\underline{\underline{F}}}$ being negative definite are sufficient to determine local stability.

Consider the following transformation of variables.

$$n = \frac{\rho C_p T}{H C_0} \qquad b = U'A + \rho C_p F_0$$

$$y = C/C_0 \qquad \tau = V/F_0$$

$$a = \rho V cp \qquad \tau_0 = \frac{\tau C_p V}{UA}$$

$$r = k(T)C \qquad U' = U/(1 + 1/F)$$

$$\hat{n} = n - n_{ss} \qquad \hat{y} = y - y_{ss}$$

$$\beta = \frac{(T_{ss} - T_{in})}{H V C_0} \qquad \hat{U}' = U' - U'_{ss}$$

$$\hat{r} = r - r_{ss}$$

Applying Krasovskii's Theorem

$$\hat{\underline{\underline{F}}} = -\begin{vmatrix} 2\left(\frac{b}{a} - \frac{1}{C_0}\frac{\partial \hat{r}}{\partial \hat{n}} + \left(\beta + \frac{n}{a}\right)A\frac{\partial \hat{U}'}{\partial \hat{n}}\right)\frac{1}{C_0}\left(\frac{\partial \hat{r}}{\partial \hat{n}} - \frac{\partial \hat{r}}{\partial \hat{y}}\right) + A\left(\beta + \frac{\hat{n}}{a}\right)\frac{\partial \hat{U}'}{\partial \hat{y}} \\ \frac{1}{C_0}\left(\frac{\partial \hat{r}}{\partial \hat{n}} - \frac{\partial \hat{r}}{\partial \hat{y}}\right) + A\left(\beta + \frac{\hat{n}}{a}\right)\frac{\partial \hat{U}'}{\partial \hat{y}} \quad 2\left(\frac{1}{C_0}\frac{\partial \hat{r}}{\partial \hat{y}} + \frac{1}{\tau}\right) \end{vmatrix}$$

The criteria for a negative definite form from Sylvester's theorem are (8):

$$\left(\frac{b}{a} - \frac{1}{C_0}\frac{\partial \hat{r}}{\partial \hat{n}}\right) + \left(\beta + \frac{\hat{n}}{a}\right)A\frac{\partial \hat{U}'}{\partial \hat{n}} > 0 \tag{23}$$

$$4\left[\frac{b}{a} - \frac{1}{C_0}\frac{\partial \hat{r}}{\partial \hat{n}} + \left(\beta + \frac{\hat{n}}{a}\right)A\frac{\partial \hat{U}'}{\partial \hat{n}}\right]\left[\frac{1}{C_0}\frac{\partial \hat{r}}{\partial \hat{y}} + \frac{1}{\tau}\right] > \left[\frac{1}{C_0}\left(\frac{\partial \hat{r}}{\partial \hat{n}} - \frac{\partial \hat{r}}{\partial \hat{y}}\right) + \left(\beta + \frac{\hat{n}}{a}\right)A\frac{\partial \hat{U}'}{\partial \hat{y}}\right]^2 \tag{24}$$

Krasovskii's boundaries and the largest Liapunov function of the form $||\underline{f}(\underline{x})||^2$ falling within Krasovskii's boundary was solved on a digital computer. These curves for various amounts of proportional control are plotted in Figures 13 and 14. Figure 13, representing the reactor without control shows that the set-point is outside Krasovskii's boundary, and therefore we cannot prove asymptotic stability. Figure 14 shows the Krasovskii's boundary for gain $K = 1.0$. The set point is within the boundary, and

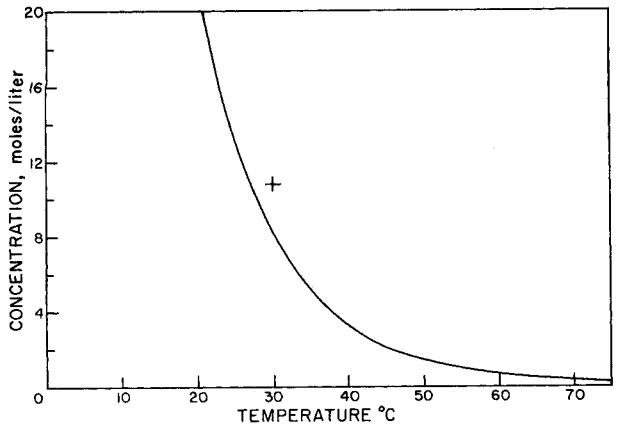


Fig. 13. Krasovskii's boundary $K = 0.0$.

fairly large Liapunov functions encircle it without exceeding the Krasovskii boundary. Comparing Figure 14 and the corresponding phase plane for the reactor without valve hysteresis (Figure 10), Krasovskii's method is seen to be conservative in predicting the region of stability. Krasovskii's method correctly predicts stability for the nonlinear system without valve hysteresis. Krasovskii's analysis cannot be applied to the system with valve hysteresis since the system must by definition have continuous first partials. This is not the case for valve hysteresis.

## CONCLUSIONS

The following conclusions are drawn on the validity of the model and evaluation of the stability analyses applied to the model.

1. In general the dynamic relationships proposed by theory must be supplemented by some experimental work. In this study the heat transfer coefficient and control valve characteristics had to be determined experimentally in order to obtain a valid model.

2. Solution of an accurate dynamic model is the most accurate and best approach for the design of a stable reactor and associated control system. The phase plane technique of representing the dynamic response for a second-order system is useful because it considers all possible initial conditions of interest, independent of time.

3. In addition to giving basic design information, the steady state approach of plotting the heat removal and heat production terms as a function of temperature determines whether or not the operating point is stable and therefore whether or not a stability analysis is necessary.

4. Neglecting valve hysteresis can lead to large errors in the results of stability predictions.

5. When valve hysteresis was not present, Krasovskii's Theorem accurately predicted regions of stability. The Liapunov function suggested by Krasovskii's Theorem (the region of assured asymptotic stability) was conservative.

6. Linearizing the nonlinear model without valve hysteresis and applying linear stability theory gave results which could not be applied to the nonlinear system.

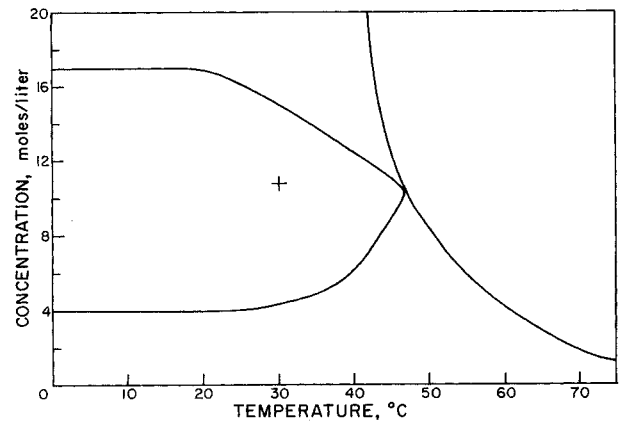


Fig. 14. Krasovskii's boundary and Liapunov function, $V(x) = ||f(x)||^2$ $K = 1$ $V(x) = 0.00022$.

## NOTATION

$A$ = reactor heat transfer area, sq.ft.
$c_p$ = specific heat, cal./g. °C.
$c$ = fraction controller output
$C$ = concentration, moles/liter
$c_1$ = constant in Equation (4)
$C_2$ = proportionality factor to convert degrees to milliamps
$C_3$ = steady state controller output in milliamps
$\hat{C}$ = $C - C_{ss}$ moles/liter
$\underline{\underline{F}}(\underline{x})$ = Jacobian matrix
$F_0$ = reactant flow liter/min.
$H$ = exothermic heat of reaction, kcal./g. mole
$k(t)$ = reaction rate constant, 1/min.
$K$ = proportional gain constant
$Q_c$ = coolant flow rate, volumetric
$r$ = rate of reaction per unit volume
$T_0$ = incoming reactant temperature, °C.
$T$ = reactor temperature, °C.
$TA$ = average coolant temperature, °C.
$T_{in}$ = incoming coolant temperature, °C.
$t$ = time in minutes
$\hat{T}$ = $(T - T_{ss})$ (°C.)
$U$ = overall heat transfer coefficient, B.t.u./hr. °F. sq.ft.
$V$ = reactor volume, liters
$V(\underline{x})$ = Liapunov function
$\underline{x}$ = state vector
$||\underline{x}||$ = Eucludian norm
$p$ = density, g./ml.

### Subscripts

ss = steady state
0 = input

### Superscripts

$\wedge$ = deviation from steady state
$T$ = transpose of a matrix
$\cdot$ = derivative with respect to time

## LITERATURE CITED

1. Aris, R., and N. R. Amundson, *Chem. Eng. Sci.*, **7**, 121 (1958).
2. Berger, J. S., and D. D. Perlmutter, *AIChE J.*, **10**, 233 (1964).
3. Bilous, O., and N. R. Amundson, *ibid.*, **1**, 513 (1955).
4. Gibson, J. E., "Nonlinear Automatic Control," Chapt. 3, McGraw Hill, New York (1960).
5. Schumb, W. C., C. N. Satterfield, and R. L. Wentworth, "Hydrogen Peroxide," pp. 189-257, Reinholt (1955).
6. Leathrum, F. S., E. F. Johnson, and L. Lapidus, *AIChE J.*, **10**, 16(1964).
7. Vanherden, C., *Ind. Eng. Chem.*, **45**, 1242 (1953).
8. West, C. J., "International Critical Tables of Numerical Data, Physics, Chemistry and Technology," p. 157, McGraw Hill, (1933).

*Manuscript received November 17, 1967; revision received May 9, 1969; paper accepted June 28, 1969. Paper presented at AIChE New York meeting.*